Numerical analysis of long period grating fibre sensor fabrication using thermal processing

S. MICLOS[a*], D. SAVASTRU[a], R. SAVASTRU[a], I. I. LANCRANJAN[a]
aNational Institute of R&D for Optoelectronics - INOE 2000, 409 Atomistilor St., Magurele, Ilfov, RO-077125, Romania

Important efforts have been and are made in studying, designing and manufacturing grating structures in single mode optical fibre. These efforts are made in order to develop all-fibre devices which can perform a transformation on the propagation of light beam (e.g. by modulating, amplifying, routing, and coupling optical signals) without extracting it from the fibre for telecommunication and sensing applications. Long Period Grating Fibre Sensors (LPGFS) form a numerous class among such all-fibre optical grating devices, being used in communications and thermal, mechanical strain and ambient refractive index (chemical) sensing. LPGFS are operated by coupling the optical power from the fundamental optical mode guided through the core into co-propagating cladding modes. LPGFS consist of a long-period grating (LPG) with 10-1000 μm spatial wavelength (period) of core refractive index modulation inscribed along the single mode fibre axis over 5 -50 mm length. LPG can be manufactured using several thermal processing techniques among which CO_2 laser local heating is a well-known and cost effective one. For being efficient these thermal processing techniques applied on optical fibres have to be computer controlled. In order to improve the design and fabrication of LPGFS development of simulation models of the thermal processes produced in optical fibre are absolutely necessary. The aim of this study consists in presenting a synthesis of results obtained into the development of optical fibre thermal processing performed for LPG fabrication.

1. Introduction

Since the optical fibres appeared in the scientific research field their possible use as sensors for various applications was intensively studied [1-5, 43-45]. The reason of this interest arose from the basic observation that any interaction of light beam propagating through an optical fibre with its ambient is potentially measurable and usable for sensing [1-5, 43-46]. Soon after first studies on use of optical fibres for sensing applications, it became clear that coupling the electromagnetic field of the light guided through the core of an optical fibre with the environment where optical fibre is placed is important for sensing applications [6-10, 43-45]. It is a contradictory situation because long distance high speed communication, which is the main optical fibre application, needs isolation as good as possible of light propagating through the optical fibre core from the environment influences [11, 12, 43-45]. For improving the sensitivity of optical fibre sensors one possibility consists in use of gratings inscribed in the optical fibre and comparatively measuring the modification of light spectrum as propagating through the core or after environment action [13-22, 43-45]. Basically, optical gratings operate by light scattering on their pitches. In the case of gratings inscribed in the optical fibre there are two possibilities: to keep the scattered light into the core,

meaning the observation of grating reflection spectrum or to couple the energy of fundamental light mode propagating through the core to other modes with possible propagation through the optical fibre cladding [13-25, 43-45]. The first case is that of Fibre Bragg Grating (FBG), the sensing function being accomplished by observation of reflection spectrum of a Bragg grating with 0.5 - 1.0 μm period inscribed in the core over a 1-5 mm length by using UV laser radiation [13-17, 43-45]. The second case is that of Long Period Grating (LPG), the sensing function being accomplished by observation of transmission spectrum of a grating with 10 - 1000 μm period inscribed in the optic fibre over a 5-50 mm length by using UV laser radiation or thermal processing techniques, including the CO_2 laser one [18-23, 25]. Use of UV laser radiation for inscribing Bragg grating or LPG in optical fibre core means creation of colour centres in the silica glass of the optical fibre [13-17, 43-45]. FBG sensors operate almost exclusively by grating period modification under mechanical or thermal environment action [13-17, 43-45]. LPG can be created not only by colour centres formation in the core of optical fibre but also by periodic modifications of optical fibre geometry by thermal processing. This is a major difference between FBG and LPG sensors in the sense that the colour centres laser UV induced in the glass of the optic fibre core for a Bragg grating fabrication have a temperature limit of around 300°C above which are becoming unstable,

disappearing. The LPG fibre sensors (LPGFS) operate not only by using LPG period modification but also by any transmission spectrum modification induced by any environment refractive index changes [18-25]. It is useful to underline that optical fibre thermal processing, including the CO_2 laser one is more effective in terms of cost compared to the UV laser technique. Also LPGFS have a larger field of applications compared to FBG fibre sensors, especially as chemical and biochemical sensors. The above considerations refer to silicate communication single mode (SM) optical fibre with a core of 4-10 µm and a cladding of 125 µm diameters, such as Corning SM 28 or Fibercore SM 750.

The main purpose of the paper consists in presenting results obtained simulation of LPGFS fabrication by using the thermal processing technique, which is common to the most financially effective (cheapest) of several ways of LPG manufacturing by optical fibre deformation: irradiation from a CO_2 laser, electric arc discharge from a commercial fibre fusion splicer, controlled flame heating and pre-heating followed by permanent mechanical deformations (bending). All these optical fibre thermal processing techniques performed in order to inscribe LPG into it have another common feature: the grating consists of periodic tapers obtained by local heating of the fibre at temperature well below the melting point combined with a slight elongation of it. It is important to underline that optical fibre is heated well below the silica glass melting point but large enough to make possible the elongation of it. The supra-cooled solution which is the silica glass is brought to the status of fluid with large viscosity coefficient [18-25]. The obtained simulation results are compared with reported in literature ones indicating a fairly good agreement.

2. Elements of theoretical model

Making LPG into single mode optical fibres by thermal processing techniques imposes, for an improved design of the optical device and of manufacturing process, a better understanding of silica glass heat absorption characteristics. CO_2 laser heating of optical fibre relies on IR properties of silica glass at a larger extent than the other thermal processing techniques [18-23, 26-28, 43-45]. The heat is absorbed inside the volume of optical fibre silica glass by absorption of CO_2 laser radiation photons and is not "migrating" from the external surface into the interior of the optical fibre. The main constituents of the optical fibre silicate glass microstructure are tetrahedral SiO_4 groups, which may be isolated as in the orthosilicates or connected with another common oxygen atom as in building a Si_2O_7 group from two connected tetrahedra. Silica has very intense absorption bands in the IR region due to linkages involving silicon. The IR properties of silica glass are correlated with the valence stretching Si-O-

Si i.e. the stretching vibration of the oxygen shared between two Si of the tetrahedral adjacent SiO_4 groups, the main basic structure constituting the silica glass. Taking into account the first two strongest absorption frequencies v_3 and v_1 of the SiO_4 structure, the degenerate and harmonic frequencies and finally the effects of the dopants, it is observed a strong absorption region in the 8.5 - 13 µm wavelength range [26-28]. In Fig. 1 are schematically presented the stretching vibration modes of oxygen of the tetrahedral adjacent SiO_4 groups. The silicate glass optic fibre heating mechanism involved when using CO_2 laser is different from that in the case of a flame. In the case of a CO_2 laser, the main part of the beam incident on the optical fibre is absorbed inside the volume of the glass because of the coupling with SiO_4 vibrational modes [18-23, 25]. The CO_2 laser beam photons create thermal excitation of the silica SiO_4 micro-crystals. The thermal excitation results in heating up the fibre but not any photon can create this effect; thermal excitation of materials is mainly stimulated by IR light situated in an overlapped relatively broad bands centred at few wavelengths, the most intense heat absorption being observed at the wavelengths defined in Fig. 1. For all the other mentioned thermal processing techniques the heat is absorbed in a thin layer at the optic fibre surface and after that is diffused into the glass volume.
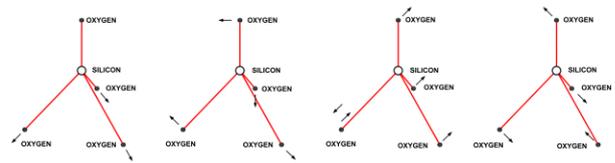
Fig. 1. The most important stretching vibration of the oxygen shared between two silicones of the tetrahedral adjacent SiO_4 groups (from left to right: $v_1 = 12.5$ µm, $v_2 = 36.4$ µm, $v_3 = 9.1$ µm, $v_4 = 21.3$ µm).

An important difference between CO_2 laser thermal processing and the other ones consists in the fact that the laser beam characteristics impose a far more accurately defined heating zone. In general, for optical fibre thermal processing, medium-low power CO_2 lasers are used [18-25]. For such a laser, the output beam with total power P_{total} can be approximated as having a Gaussian transverse intensity distribution with good quality, meaning that it has a M^2 factor almost equal to 1, $I(x,y)$, which is defined as in Equation (1), where w_x and w_y are the laser beam waists on the coordinate axis. The previously mentioned M^2 factor is the beam quality factor, measuring the deviation of the actual CO_2 laser beam intensity transverse distribution from an ideal Gaussian one. For a small slice δx in the x direction, the incident CO_2 laser power falling on the fibre is defined as in (2).

$$I(x,y) = \frac{2P_{Total}}{\pi w_x w_y} \exp\left[-2\left(\frac{x^2}{w_x^2} + \frac{y^2}{w_y^2}\right)\right] \quad (1)$$

$$\delta W = \frac{P_{Total}}{w_x \sqrt{\pi}} erf\left(\frac{d\sqrt{2}}{w_y}\right) \exp\left(-2\frac{x^2}{w_x^2}\right)\delta x \quad (2)$$

The laser output beam is focused at normal incidence on optical fibre axis to an elliptic shape spot. The laser output beam uses simple focusing optics [29, 30]. The small slice δx in the x direction is defined as in Equation (2). δx in Fig. 2 represents the portion of the optical fibre which is illuminated by the CO_2 laser beam. The two coordinate axes introduced in Equations (1) and (2) and in Fig. 2 are usually defined one along the optic fibre (the x axis) and the other perpendicular to it (the y axis).
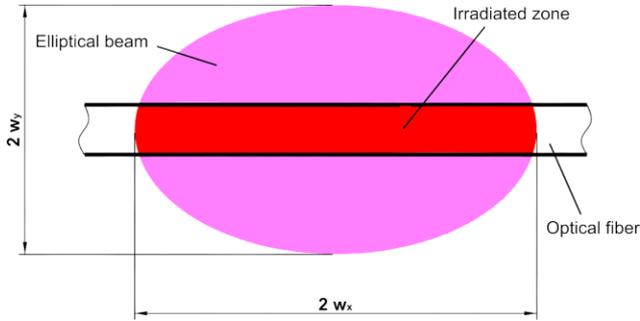
Fig. 2. Irradiation geometry.

It is useful to underline another important difference between the CO_2 laser beam thermal processing techniques and the other enumerated ones applied on optical fibre for LPG fabrication. This difference arose from the possibility to use the old approximatively geometrical ray theory in order to obtain information about which part of the incident CO_2 laser power is reflected, absorbed or transmitted by the optical fibre [18-23, 25].
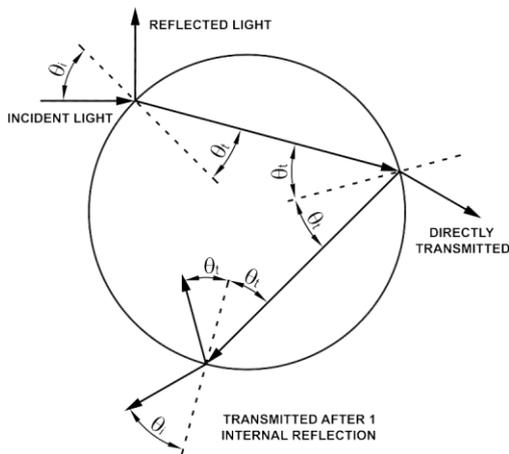
Fig. 3. Ray theory model.

This is not possible for the other enumerated heat processing techniques applied on optical fibres for LPG fabrication. In Fig. 3 can be observed the schematic representation of the application of ray theory model where one and/or two internal reflections occur at the interface optic fibre and air [31, 32].

A rigorous analysis imposes that separate calculations for the parallel and the perpendicular component of the incident electric field are performed. Because the optical fibre surface is curved and the CO_2 laser is not a point source but it is approximated as a plane wave having a Gaussian intensity profile incident on the fibre. The reflected and absorbed power needs to be computed for an incident angle between 0 and 90°. Application of ray theory makes possible the calculation of real and imaginary parts of glass complex refractive index, m. The imaginary part of m, denoted as k, is an important parameter constant which will be used in the heat transfer equation, the key equation of the developed simulation model of thermal processing techniques applied on optic fibre for LPG manufacturing. Fig. 4 schematically presents an equivalent procedure for application of ray theory.
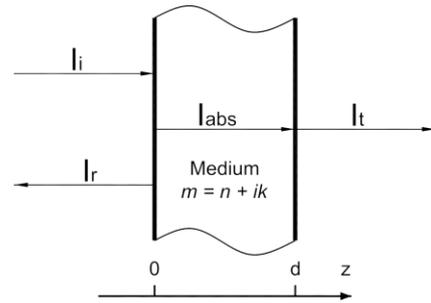
Fig. 4. Slab transmission and reflection, m – complex refraction index.

A specific issue of thermal processing applied on optical fibre for LPG fabrication arise from the geometry of the target. Optical fibre can be considered as a wire illuminated by a controlled shuttered up and down CW CO_2 laser beam or heated from a flame or electric arc discharge during periods of few seconds, this being the usual experimental procedure. A longer heating period can cause glass wire melting. A too short heating period has no effect or an insignificant effect on the optical fibre. The analysed specific issue is defined as thermal thinness condition. It is connected to the silica glass thermal time constant which has a value of 2.03 μs, much shorter than the usual experimental exposure time of optical fibre to the heat source. The thermal thinness condition is fulfilled in the cases of CO_2 laser, flame, electric arc discharge heat sources. The silica glass thermal time constant means the time necessary for heat diffusion, measured by temperature, from a point source to $1/e^2$ into a semi-infinite material. Accordingly, in the heating zone, the

optical fibre temperature is considered uniform throughout its thickness. Therefore, the analysed problem can be reduced to a 1-D heat transfer in the case of an optical fibre subjected to thermal processing.

In the followings the analysed experimental setups are presented in order to underline the common characteristics and the differences. The first one is the schematic of the experimental setup of LPGFS fabrication using a CO_2 laser as heating source which is presented in Fig. 5 [4, 5, 16, 19, 20, 25]. A point-by-point procedure is used, which is common to the investigated setups. The pitches of the fibre grating are made one-by-one by CO_2 laser heating for a predefined time interval of few seconds. For manufacturing of the entire grating the optical fibre has to be translated (almost all of the cases) or the laser beam is put on successive positions using a scanning mirror (a procedure rarely used). The LENS in Fig. 5 represents the CO_2 laser beam focusing system which can transform the spot of Fig. 2 into a much distorted ellipse with main axis perpendicular to optical fibre axis. The elongation of optical fibre is obtained by pulling it with small weights (1-10 g).
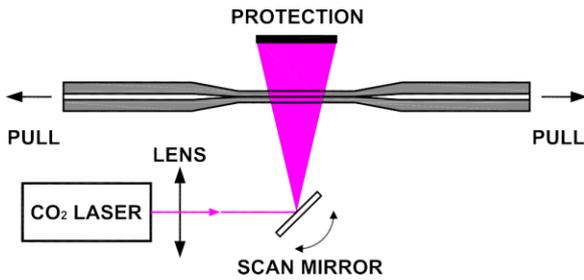
Fig. 5. Schematic of LPGFS fabrication setup

In Fig. 6 is presented the setup used in the case of air electric arc discharges. An uncoated fibre is placed between the electrodes of a fusion splicing machine (electrodes gap = 0.9 - 1.0 mm, electrodes apex angle = 20 - 40°) [6, 7, 10, 47]. One end of the fibre is clamped in a fibre holder on top of a motorized translation stage controlled with a precision of 0.1 μm. At the other end a weight is attached to keep the fibre under a constant axial tension (1 - 40 g). An arc discharge is then produced with an electric current of 8.5 - 10 mA during 0.5 – 2 s exposing a short portion of the length of fibre. As in the case of laser CO_2 thermal processing, the optical fibre is heated the procedure for LPG fabrication is accomplished in a simple logical way: the optical fibre is heated up to the few seconds being softened to the level where a taper of the optic fibre is produced by elongation induced by the attached small weigh, after the heating is stopped, the optical fibre is computer controlled longitudinally translated; when it is in a fixed position the heating process is repeated and so on until the entire grating is fabricated.
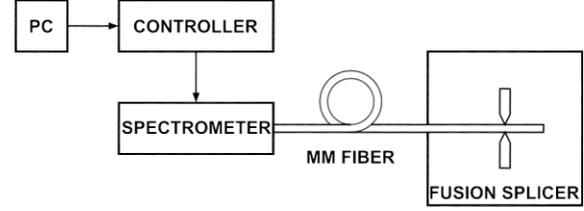
Fig. 6. Point-by-point LPGFS fabrication setup

Fig. 7 presents the optical fibre thermal processing by flame heating. An uncoated fibre is exposed to the flame generated by a gas burner which uses premixed ultraclean hydrogen and oxygen to avoid pollution of the optical fibre [17]. The maximum temperature of the oxygen-hydrogen flame is as high as 3050°C. One end of the fibre is clamped in a fibre holder on top of a motorized translation stage controlled with a precision of 0.1 μm. At the other end a weight is attached to keep the fibre under a constant axial tension (1-40 g).
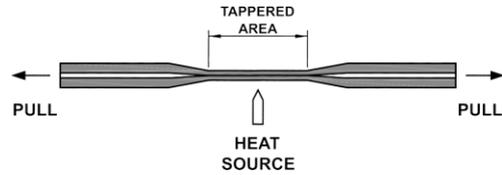
Fig. 7. Setup for optical fibre processing by flame heating

The experimental setups presented schematically in Figs. 5, 6 and 7 have a common characteristic which is the main equation to be solved. After some calculations the following thermal transfer equation is defined as [17]:

$$\frac{\partial T}{\partial t} = \frac{1}{\rho c}\left[K\frac{\partial^2 T}{\partial x^2} + \frac{4H}{d}\left(T_{air} - T\right) + \frac{4\sigma\varepsilon}{d}\left(T_{air}^4 - T^4\right) + q(x)\right] \quad (3)$$

where T and T_{air} are the optical fibre and ambient air temperatures; ρ is the silica glass density, σ is the Stefan-Boltzmann constant, ε is the silica glass emissivity, c is the silica glass specific heat, K is the silica glass thermal conductivity, H is the coefficient of silica glass heat transfer (also known as surface conductance), and d is the optic fibre diameter. In Equation (3) these constants are defined as temperature functions. In Equation (3) the term $q(x)$ represents the CO_2 laser heat source.

3. Simulation results

The development of the simulation model was conducted in two principal stages. The first stage consisted in defining as accurate as possible constants used in Equation (3). In the second stage Equation (3) is solved. Equation 3 is a partial derivative equation which has as a solution a function $T(x,t)$, x being the distance along the

optic fibre from the CO_2 laser beam incidence point, the point of intersection of laser beam axis with the optic fibre surface. The solution $T(x,t)$ describes the time and space variation of optical fibre temperature. In deriving Equation (3) the initial and border conditions concerning T were observed. The initial conditions are the same for the three analysed thermal processing techniques applied to optical fibres and can be expressed by a simple condition, at $x = 0$ the heating source is on for a previously defined time or off. The border conditions are also the same for the three analysed thermal processing techniques, namely T is equal to T_{air} at large x positive or negative values. As a result, the temperature distribution along the optical fibre is obtained solving Equation (3). In the first stage of simulation model development, the coefficients used in Equation (3) are defined, if necessary as function of temperature (T). In Figs. 8, 9, 10 and 11 there are presented the variation with temperature of silica glass specific heat [33-36], air thermal conductivity [37-39], silica glass thermal conductivity [40-42] and silica glass heat transfer [36-42]. In Fig. 8 is presented the silica glass specific heat variation with T [33-36].
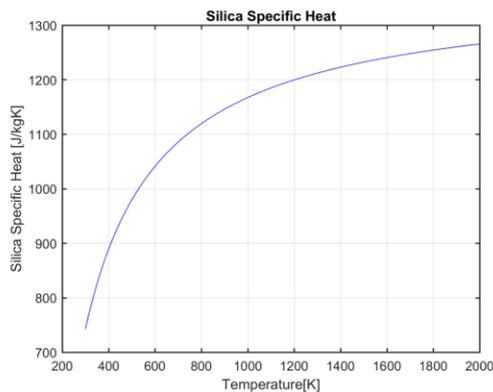
Fig. 8. Silica glass specific heat variation with temperature

In Fig. 9 is presented the variation versus ambient temperature of air, K_{air} [40-42]. This parameter is important as measuring the possible transfer of heat from the locally heated optic fibre to the ambient air (atmosphere).
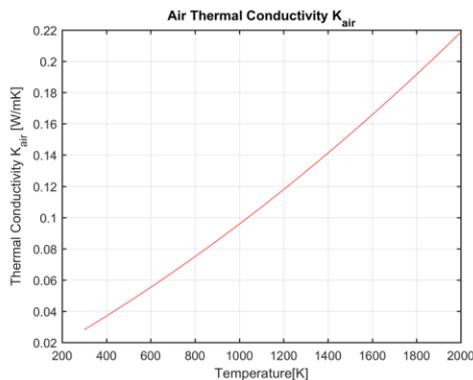
Fig. 9. Air thermal conductivity variation with temperature

In Fig. 10 is presented the variation versus ambient temperature of silica glass thermal conductivity as being placed in air, K_{silica} [32, 40-42]. This parameter is important as measuring the possible transfer of heat from the locally heated optic fibre to the ambient air (atmosphere).
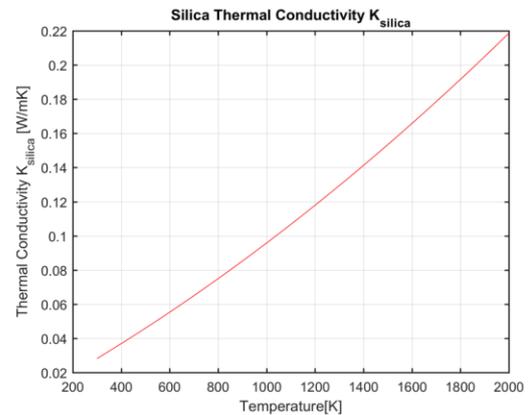
Fig. 10. Silica glass thermal conductivity variation with temperature.

In Fig. 11 is presented the variation versus ambient temperature of silica glass heat transfer coefficient as being placed in air, H [33, 34, 40-42]. This parameter is important as measuring the possible transfer of heat from the locally heated optic fibre to the ambient air (atmosphere).
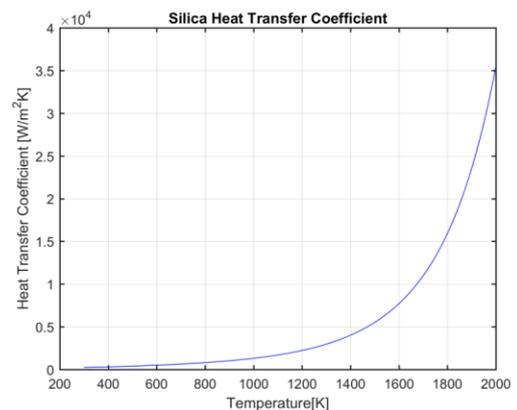
Fig. 11. Silica glass heat transfer coefficient variation with temperature

The simulation of optical fibre thermal processing for fabrication of LPGFS has the heat transfer equation as the main issue. In Fig. 12 and 13 are presented, as examples, the simulation results obtained in the case of standard silica SM optical fibre with a diameter of 125 μm CO_2 laser thermal processed. The simulation results were obtained considering an elliptic laser spot (0.5 mm length of the secondary axis) on the optical fibre with a CW power of 2.8 W. There were considered two CO_2 laser

primary axis orientations: parallel and perpendicular on the optical fibre axis (in Figs. 12 and 13 perpendicular orientation is presented). It was analysed the case of applying CO_2 laser power instantly at $t = 0$, with no rise time. It is worth to be noticed that in less than a second the optic fibre is stabilized at a high temperature of 2000 K, near the melting point.
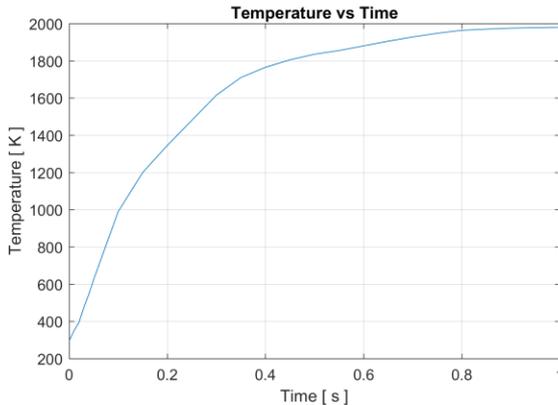
Fig. 12. Evolution of the fibre temperature vs. time

Fig. 13 presents the simulated equilibrium temperature distribution along the fibre considering thermal processing CO_2 laser beam spot with main axis perpendicular to optical fibre axis. The simulation results were obtained considering an elliptic laser spot with the secondary axis of 0.5 mm length on the optical fibre at a CW output power of 2.8 W. The peak CO_2 laser beam intensity was considered as incident on optical fibre at $x = 0$. The temperature distribution was symmetric for negative x values, being a mirror reflection of the presented curve.
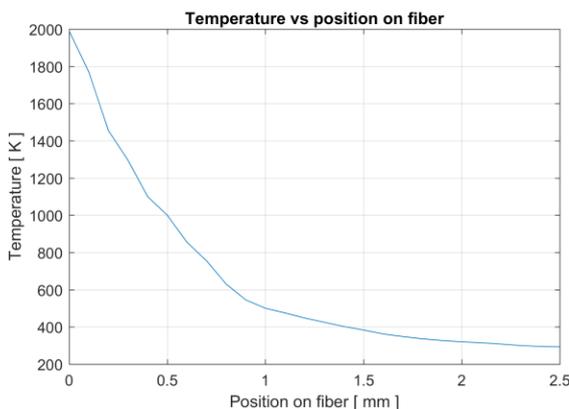
Fig. 13. Evolution of the temperature along the fibre at the equilibrium temperature

4. Conclusions

The results obtained in simulation of optical fibre thermal processing for manufacturing using different

procedures of LPGFS are presented. The presented results are in fair good agreement with the simulation or experimental ones reported in literature. The presented simulation results are aiming to improve the LPGFS design in order to extent the dynamic measuring range and accuracy of this type of sensors used for various applications.

References

[1] B. Lee, Opt. Fiber Technol. **9**, 57 (2003).
[2] S. W. James, R. P. Tatam, Meas. Sci. Technol. **14**, R49 (2003).
[3] A.D. Kersey, M. A. Davis, H. J. Patrick, M. LeBlanc, K. P. Koo, C. G. Askins, et al., J. Lightwave Technol. **15**, 1442 (1997).
[4] L. Gallais, P. Cormont, J. Rullier, Opt. Express **17**, 23488 (2009).
[5] S. Z. Xu, X. T. Zu, X. D. Yuan, Chinese Opt. Lett. **9**, 061405 (2011).
[6] G. Humbert, A. Malki, J. Opt. A: Pure Appl. Op. **4**, 194 (2002).
[7] P. Palai, M. N. Satyanarayan, M. Das, K. Thyagarajan, B. P. Pal, Optics Commun. **193**, 181 (2001).
[8] A. Dragomir, D. N. Nikogosyan, A. A. Ruth, K. A. Zagorul'ko, P. G. Kryokov, Electron. Lett. **38**, 269 (2002).
[9] H. J. Qi, M. P. Zhu, M. Fang, S.Y. Shao, C.Y. Wei, K. Yi, et al., High Power Laser Sci. Eng. **1**, 36 (2013).
[10] G. Rego, O. Okhotnikov, E. Dianov, V. Sulimov, J. Lightwave Technol. **19**, 1547 (2001).
[11] J. Canning, Opt. Fiber Technol. **6**, 275 (2000).
[12] M. Fujimaki, Y. Ohki, J. L. Brebner, S. Roorda, Opt. Lett. **25**, 88 (2000).
[13] M. A. Norton, E. E. Donohue, W. G. Hollingsworth, M. D. Feit, A. M. Rubenchik, R. P. Hackel, Proceedings SPIE **5647**, 197 (2005).
[14] D. Savastru, S. Miclos, R. Savastru, I. Lancranjan, Rom. Rep. Phys. **67**, 1586 (2015).
[15] G. D. Tsibidis, M. Barberoglou, P. A. Loukakos, E. Stratakis, C. Fotakis, Phys. Rev. B **86**, 115316 (2012).
[16] D. D. Davis, T. K. Gaylord, E. N. Glytsis, S. C. Mettler, Electron. Lett. **34**, 1416 (1998).
[17] J. R. M. Vignes, T. F. Soules, J. S. Stolken, R. R. Settgast, S. Elhadj, M. J. Matthews, J. Am. Ceram. Soc. **96**, 137 (2013).
[18] A. J. C. Grellier, N. K. Zayer, C. N. Pannell, Opt. Commun. **152**, 324 (1998).
[19] L. Drozin, P.-Y. Fonjallaz, L. Stensland, Electron. Lett. **36**, 742 (2000).

[20] F. Keilmann, Y. H. Bai, Appl. Phys. A **29**, 9 (1982).
[21] K. F. Ren, G. Grehan, G. Gouesbet, J Opt Soc Am A **14**, 3014 (1997).
[22] A. E. Siegman, P. M. Fauchet, IEEE J. Quantum Elect. 22, 1384 (1986).
[23] J. E. Sipe, H. M. van Driel, P. Soc. Photo-Opt. Inst. **1033**, 302 (1988).
[24] P. E. Dyer, R. J. Farley, R. Giedl, D. M. Karnakis, Appl. Surf. Sci. **96**–**98**, 537 (1996).
[25] R. Diaz, M. Chambonneau, R. Courchinoux, P. Grua, J. Luce, J.-L. Rullier, et al. Opt. Lett. **39**, 674 (2014).
[26] T. A. Birks, Y. W. Li, J. Lightwave Technol. **10**, 432 (1992).
[27] R. P. Kenny, T. A. Birks, K. P. Oakley, Electron. Lett. **27**, 1654 (1991).
[28] M. D. Crisp, N. L. Boling, G. Dubé, Appl. Phys. Lett. **21**, 364 (1972).
[29] N. Hodgson, H. Weber, Laser Resonators and Beam Propagation. Fundamentals, Advanced Concepts and Applications, 2nd ed. New York: Springer Science + Business Media Inc.; 2005.
[30] A. E. Siegman, Lasers, Sausalito, California: University Science Books, 1986.
[31] E. D. Palik, Handbook of optical constants of solids. Orlando: Academic Press, 1985.
[32] R. Brückner, J. Non-cryst. Solids **5**, 123 (1970).
[33] J.P. Holman, Heat transfer. 2nd Edition. New York:Mc Graw-Hill;1968.
[34] E. Bar-Ziv, A. F. Sarofin, Prog. Energy Combust. **7**, 1 (1991).

[35] Y. S. Touloukian, C. Y. Ho, Thermophysical Properties of matter: The TPRC data series, vol. 5: Specific heat – nonmetallic solids, Purdue University 1979.
[36] Heraeus Silica and Metals Ltd., Physical characteristics of silica. 96/97 catalog, 4-11 to 4-14, 1996.
[37] O. V. Mazurin, M. V. Streltsina, T. P. Shvaiko-Shvaikovskaya, Physical Sciences Data ISA, Handbook of glass data, Part A: Silica glass and binary silicates glasses. Elsevier, 1983.
[38] I. Langmuir, Phys. Rev. **34**, 401 (1912).
[39] B. Gebhart, Heat transfer. McGraw-Hill, 1971.
[40] F. Kreith, Principles of heat transfer. 2nd ed., Scranton:International Textbook Co., 1965.
[41] W. Elenbass, J. App. Physics **19**, 1148 (1948).
[42] W. H. McAdams, Heat transmission. 3rd Edition. New York: McGraw-Hill, 1954.
[43] I. Lancranjan, S. Miclos, D. Savastru, A. Popescu, J. Optoelectron. Adv. M. **12**, 2456 (2010).
[44] I. Lancranjan, S. Miclos, D. Savastru, J. Optoelectron. Adv. M. **12**, 1636 (2010).
[45] S. Miclos, D. Savastru, I. Lancranjan, Rom. Rep. Phys. **62**, 519 (2010).
[46] I. Navruz, M. Bilsel, F. Ari, J. Optoelectron. Adv. M. **19**, 486 (2017).
[47] D. Liu, G. Humbert, Y. Liu, D. Zhao, Optoelectron. Adv. Mat. **11**, 289 (2017).

_____

[*]Corresponding author: miclos@inoe.ro